RSC Advances

ROYAL SOCIETY OF CHEMISTRY

www.rsc.org/advances

Effect of different donor group in bis(6-methoxylpyridin-2-yl) substituted co-sensitizer on the performance of N719 sensitized solar cells

Liguo Wei,[ab] Yulin Yang,*[a] Zhaoyang Zhu,[ac] Ruiqing Fan,*[a] Ping Wang,[a] Yuwei Dong[a] and Shuo Chen[a]

[a] *Department of Chemistry, Harbin Institute of Technology, Harbin 150001, P.R. China.*

[b] *College of Environmental and Chemical Engineering, Heilongjiang University of Science and Technology, Harbin 150022, P.R. China.*

[c] *Hubei Institute of Aerospace Chemotechnology, Xiangyang 441003, P.R. China.*

To whom the correspondence should be addressed.

Prof. Yulin Yang and Ruiqing Fan

Department of Chemistry, Harbin Institute of Technology, Harbin 150001, P. R. China

Fax: +86-451-86418270

E-mail: ylyang@hit.edu.cn and fanruiqing@hit.edu.cn

Three bis(6-methoxylpyridin-2-yl) substituted pyridine-anchor co-sensitizers with different donor group are synthesized by 1,2-diaminobenzene (named L4), 1,2-diaminocyclohexane (named L5) and 1,4-butanediamine (named L6) with the aim to obtain rigid, semi-rigid and flexible co-sensitizer molecules, respectively. Their adaptability in N719 sensitized solar cells as co-sensitizer and the effects of their molecular rigidity, conjugation and co-planarity on the performance of DSSCs are studied. The results show that these three co-sensitizers are suitable to use in N719 sensitized solar cells. However, due to the different donor group in molecular structure, the co-sensitization performance of the rigid co-sensitizer with large conjugate system is better than that of semi-rigid and flexible co-sensitizers. A short circuit current density of 13.27 mA cm^{-2}, an open circuit voltage of 0.73 V and a fill factor of 0.63 corresponding to an overall conversion efficiency of 6.16% under AM 1.5G solar irradiation were achieved when rigid L4 was used as co-sensitizer, which is 30% higher than that for DSSCs only sensitized by N719 (5.37%) under the same condition. Mechanistic investigations are carried out by various spectral and electrochemical characterizations.

1. Introduction

Dye-sensitized solar cells (DSSCs) have attracted much attention due to their low-cost production, non-vacuum process, environment friendly energy conversion, and fairly high performance since the outstanding breakthroughs made by the Grätzel group.[1-3] However, much improvement in efficiency is desired for these devices before they could take place of the Si based solar cells. Therefore, research groups all over the world have provided several strategies to improve the photovoltaic performance of ruthenium dye sensitized solar cells, among which co-sensitization is considered to be a more promising way to combine the spectral responses of co-sensitizer on the film for performance enhancement.[4-6] For example,

Han and Arakawa obtained a high efficiency of above 11.0% by co-sensitization of the black dye with organic compounds, respectively.[7,8] Dehghani co-sensitized N719 dye with a porphyrin dye ZnTCPP, resulting in the efficiency of 6.35%, which was higher than that of 4.75% based on N719 alone.[9] Holliman co-sensitized N719 dye with triarylamine dyes, DSSC efficiency of 7.5% has been achieved which exceeds those records for individual dye devices.[10] Yang reported a co-sensitized system using N719 dye with metal-free organic dye FL. The cell efficiency was optimized to be 5.10%, which was higher than that of the cell soaking only in N719 (4.89%).[11] Ko published a co-sensitization study using Ru-complex JK-142 and organic JK-62 dye. The DSSC efficiency exhibited 10.2% surpassing that of cells using only JK-142 dye (7.28%) or JK-62 dye (5.36%).[12] Sharma obtained a cell efficiency of 7.35% by co-sensitization of zinc-porphyrin and thiocyanate-free ruthenium(II) terpyridind dyes.[13] Wu co-sensitized N719 with an organic dye resulting in an efficiency of 7.91%, 8.6% higher than that of N719 sensitized alone.[14] Chang reported efficient panchromatic light harvesting by co-sensitization of a porphyrin molecule and N719 in dye sensitized solar cells, the co-sensitized devices shows a considerably enhanced power conversion efficiency of 8.89%, higher than individually sensitized by N719.[15] However, the select of co-sensitizer is very important in this co-sensitization. Usually, most groups focus on synthesis co-sensitizers with one or more carboxyl-anchor group. While recently co-adsorbents containing pyridine-anchor unit instead of the conventional carboxyl-anchor group is prove to be effective in co-sensitized DSSCs and these pyridine-anchor dyes were confirmed to adsorb preferentially at the Lewis acid sites of the TiO_2 surface (the sites of exposed Ti atoms) and they can also adsorb at the Brønsted acid sites of the TiO_2 surface if the Brønsted acid sites are not occupied, which explore a new type of co-sensitizer in

improving the performance of DSSCs.[16-19] In the previous work of our group, N,N'-Bis((6-methoxylpyridin-2-yl) methylene)-*p*-phenylenediimine and its transition metal complexes were employed in N719 sensitized solar cells and were proved to be promising candidates for highly efficient co-sensitized solar cells.[20,21] In this kind of co-sensitizer molecule, the donor group locates on the *p*-phenylenediimine group and the pyridine ring works as acceptor group. The effect of different acceptor group on the performance of co-sensitized solar cell was investigated before and the 6-methoxylpyridin group was shown to be a better one. However, the effect of different donor group on the performance of co-sensitized solar cell were still unknow.

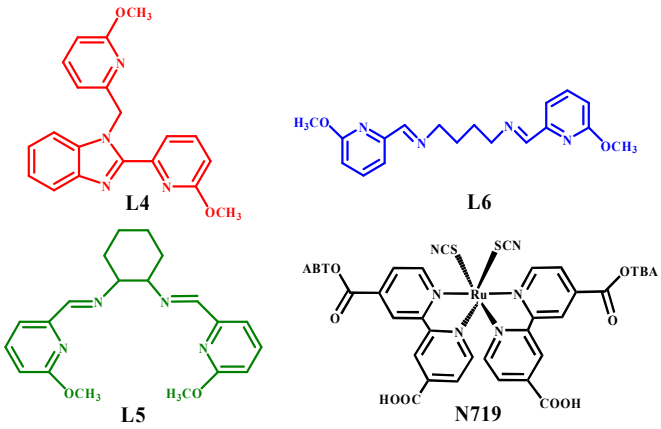

Scheme 1 Molecular structures of L4, L5, L6 and N719.

Therefore, in this work, three bis(6-methoxylpyridin-2-yl) substituted pyridine-anchor co-sensitizers with different donor group are synthesized by 1,2-diaminobenzene (named L4, Scheme 1), 1,4-diaminocyclohexane (named L5, Scheme 1) and 1,4-butanediamine (named L6, Scheme 1) with the aim to obtain rigid, semi-rigid and flexible co-sensitizer molecules, respectively. Their adaptability in N719 (Scheme 1) sensitized solar cells as co-sensitizer and the effects of their molecular rigidity on the performance of DSSCs are studied. The results show that these co-sensitizers are suitable to use in N719 sensitized solar cells. However,

due to the different donor group in molecular structure, the co-sensitization performance of the rigid co-sensitizer with large conjugate system is better than that of semi-rigid and flexible co-sensitizers.

2. Experimental section

2.1 Materials

The FTO conducting glass (Fluorine-doped SnO_2, sheet resistance 15 Ω per square, transmission 90% in the visible range) was purchased from NSG, Japan, and cleaned by a standard procedure. N719 [Bis-tetrabutylammonium cis-bis(isothiocyanato)bis(2,2-bipyridyl -4,4-dicarbox-ylato)ruthenium(II)] was purchased from Solaronix Company, Switzerland. All of the other solvents and chemicals used in this work were of reagent grade without further purification. And all characterizations were carried out under ambient pressure and room temperature.

2.2 Synthesis of L4, L5 and L6

The compound L4 was synthesized according to the following method: 6-Methoxypyridine-2-carbaldehyde (20 mmol, 2.406 g) was drop-wise added to a mixture of 1,2-diaminobenzene (10 mmol, 1.10 g) and methanol (20 mL). The mixture was heated and refluxed for 24 h, then cooled down, filtrated out the yellow powder and recrystallized with hexane. Then the white clump sample of L4 was obtained (1.60 g, 45 %). ^{1}H NMR (400 MHz, DMSO-d_6, ppm): δ = 8.00 (d, 1H, *J* = 7.2 Hz, Py-*H*), 7.87 (d, 1H, *J* = 7.2 Hz, Py-*H*), 7.77 (dt, 1H, *J* = 3.6, 6.4 Hz, Py-*H*). 7.62 (dt, 1H, *J* = 4.0, 7.2 Hz, Py-*H*), 7.53 (t, 1H, *J* = 8.0 Hz, Py-*H*), 7.28 (dt, 2H, *J* = 3.6, 6.4 Hz, Py-*H*, Ph-*H*), 6.89 (d, 1H, *J* = 8.0 Hz, Ph-*H*), 6.61 (d, 1H, *J* = 8.4 Hz, Ph-*H*), 6.42 (d, 1H, *J* = 7.2 Hz, Ph-*H*), 6.22 (s, 2H, CH_2), 3.68 (s, 3H, OCH_3), 3.63 (s, 3H, OCH_3). FT-IR (KBr, cm^{-1}): 3446 (m), 3050 (m), 2949 (m), 2860 (w),

1588 (s), 1471 (s), 1442 (s), 1391 (m), 1316 (m), 1266 (m), 1073 (m), 1027 (m), 901 (s), 746 (s), 431 (s). UV-vis (nm, in methanol, 25 ºC): 232, 279, 319. Elemental analysis for $C_{20}H_{18}N_4O_2$ (M_r: 346.39): calcd. C, 69.35%; H, 5.24%; N, 16.17%. found C, 69.58%; H, 5.12%; N, 16.39%.

The synthesis procedure of L5 and L6 were the same as that for L4 except that 1,2-diaminobenzene was replaced by 1,2-diaminocyclohexane (10 mmol, 1.202 ml) and 1,4-butanediamine (10 mmol, 1.002 ml), respectively. The synthesis of L4, L5 and L6 are summarized in Scheme 2.

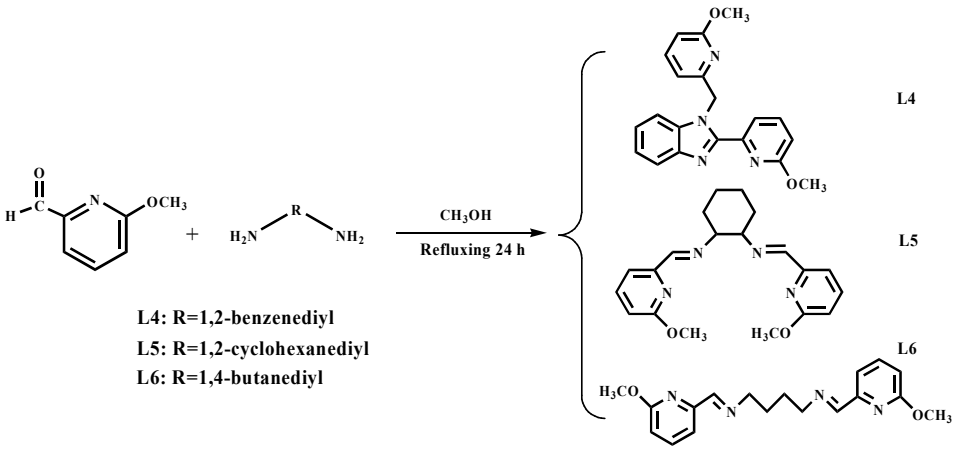

Scheme 2 Synthesis routes of L4, L5 and L6.

L5 (2.60 g, 74 %): ^{1}H NMR (400 MHz, DMSO-d_6, 298 K, TMS): δ = 8.12 (s, 2H, C*H*=N), 7.66 (t, 2H, *J* = 8.0 Hz, Py-*H*), 7.45 (d, 2H, *J* = 7.2 Hz, Py-*H*). 6.81 (d, 2H, *J* = 8.4 Hz, Py-*H*), 3.84 (d, 2H, *J* = 9.4 Hz, Cy-C*H*), 3.77 (s, 6H, OCH_3), 1.77 (m, 6H, Cy-CH_2), 1.45 ppm (t, 2H, *J* = 8.8 Hz, Cy-CH_2). FT-IR (KBr, cm^{-1}): 3086 (m), 2992 (w), 2945 (s), 2860 (s), 1653 (vs), 1575 (s), 1473 (s), 1032 (s), 987 (m), 812 (s), 660 (m). UV-vis (nm, in CH_2Cl_2, 25 ºC): 230, 297. Elemental analysis for $C_{20}H_{24}N_4O_2$ (M_r: 352.43): calcd. C, 68.16%; H, 6.86%; N, 15.90%. found C, 68.30%; H, 6.64%; N, 16.15%.

L6 (4.78 g, 73 %): ^{1}H NMR (400 MHz, $CDCl_3$, 298 K, TMS): δ = 8.28 (s, 2H, C*H*=N),

7.61 (dt, 4H, *J* = 7.6, 12.8 Hz, Py-*H*), 6.75 (d, 2H, *J* = 7.6 Hz, Py-*H*), 3.97 (s, 6H, OCH_3), 3.73 (t, 4H, 4H, *J* = 7.6 Hz, CH_2), 1.81 ppm (m, 4H, CH_2). FT-IR (KBr, cm^{-1}): 3050 (m), 2992 (w), 2940 (m), 2846 (s), 1646 (vs), 1591 (s), 1470 (s), 1031 (m), 981 (m), 806 (vs), 726 (s), 633 (s). UV-vis (nm, in CH_2Cl_2, 25 ºC): 242, 296. Elemental analysis for $C_{18}H_{22}N_4O_2$ (M_r: 326.40): calcd. C, 66.24%; H, 6.79%; N, 17.17%. found C, 66.26%; H, 6.91%; N, 17.25%.

2.3 Fabrication of Devices

TiO_2 paste for screen printing was prepared according to the literature.[22] It was printed onto conductive glass (FTO, 15 Ω $sq.^{-1}$, 90% transmittance in the visible, NSG, Japan) and then dried at 100 ºC for 5 min. The above process was repeated for six times. The obtained TiO_2 film was then sintered at 500 ºC for 15 min. Co-sensitization of the TiO_2 film was accomplished by dipping it in various solutions for different time intervals at room temperature. Typically, the photoanode was immersed in a solution of 0.3 mM L4 in absolute ethanol for 2 h and then washed with ethanol. It was further immersed in a solution of 0.3 mM N719 in absolute ethanol for 12 h and then washed with ethanol. The sandwich-type solar cell device was assembled by placing a platinum-coated conductive glass as counter electrode on the co-sensitized photoanode, a drop of liquid electrolyte containing 0.5 M LiI, 0.05 M I_2, 0.1 M 4-tert-butylpyridine (TBP) was added to fill the void between two electrodes and clipped together as open cells for measurement.

2.4 Instrumentation and Measurements

UV-visible absorption spectra were recorded on SPECORD S600 spectrophotometer (Jena, Germany) for samples in ethanol solution and UV-2250 spectrophotometer (Shimadzu, Japan) for sensitized TiO_2 films, respectively. Fluorescence properties of the synthesized

compounds were obtained using an FLS920 spectrometer (Edinburgh) equipped with a peltier-cooled R928 photomultiplayer tube (Hamamatsu). A Xe900 450 W Xenon arc lamp was used as exciting light source. Cyclic voltammetry were recorded using a CHI660D electrochemical potentiostat. The measurements were carried out in a three-electrode cell under argon. The working electrode was a planar platinum working electrode and the auxiliary electrode was a platinum wire. The reference electrode was a saturated calomel reference electrode in saturated KCl solution. A solution of 0.1 M $TBAPF_6$ in dry ethanol was used as electrolyte. Photocurrent-photovoltage (*I-V*) curves were recorded by Keithley model 2400 digital source meter under AM1.5G irradiation. The incident light intensity was 100 mW cm^{-2} calibrated by a standard silicon solar cell. The working areas of the cells were masked to 0.16 cm^{-2}. Based on *I-V* curve, the fill factor (*FF*) is defined as: $FF = (J_{max} \times V_{max})/(J_{sc} \times V_{oc})$, where J_{max} and V_{max} are the photocurrent density and photovoltage for maximum power output; J_{sc} and V_{oc} are the short-circuit photocurrent density and open-circuit photovoltage, respectively. The overall energy conversion efficiency η is defined as: $\eta = (FF \times J_{sc} \times V_{oc})/P_{in}$ where P_{in} is the power of the incident light. The amounts of absorbed dye were measured by desorbing the dye from the dye-sensitized films in a 0.1 M NaOH solution in water and ethanol (1:1, V/V), and then the concentration of desorbed dye in the NaOH solution was measured using an UV-visible spectrophotometer. The measurement of the incident photon-to-current conversion efficiency (IPCE) was performed by an EQE/IPCE spectral response system (Newport). Transient absorption (TA) system was based on an amplified Ti: sapphire laser combined with an optical parametric amplifier to obtain excitation light at 532 nm and white-light continuum generation optics to obtain probe light. The light beams were focused on the DSSC under open-circuit conditions from the

transparent conductive glass side, and diffusely reflected light was collected by an achromatic lens (80 mm focal length, 50 mm diameter) to relay the probe light to an InGaAs photodetector (Thorlabs, PDA10CS) through a monochromator (Acton Research, SpectraPro-150). EIS were recorded by CHI660D Electrochemical Analyzer (Chenhua, China), and the measurements were taken over a frequency range of 0.1-100 kHz under standard global AM1.5 solar irradiation (100 mW cm^{-2}) or in the dark by applying a forward bias of -0.75V. Open-circuit voltage decay curves (OCVD) and dark current were also recorded by CHI660D Electrochemical Analyzer. ^{1}H NMR (400 MHz) spectra were recorded on a Bruker Avance-400 spectrometer using $Si(CH_3)_4$ as an internal standard at room temperature. Infrared spectra (IR) were obtained from KBr pellets on a Nicolet Avatar-360 Ingrared spectrometer in the 4000-400cm^{-1} region. Elemental analyses were performed on a Perkin-Elmer 2400 element analyzer.

3. Results and discussions

3.1 Optical properties of L4, L5 and L6

The absorption spectra of L4, L5 and L6 in ethanol and on film are shown in Fig. 1 and its absorption data are listed in Table 1. In ethanol solution (Fig. 1a), all of the three prepared compounds display strong absorption peaks in the region of 250-350 nm, which is attributed to intramolecular charge transfer (ICT). Compared with the absorption spectrum of N719, apparently, the absorption spectra of L4, L5 and L6 could compensate for that of N719 in the low wavelength region of visible spectrum, especially in the region of 300-350 nm for L4 and 250-300 nm for L5 and L6. Furthermore, as shown in Table 1 the molar extinction coefficients of L4, L5 and L6 in the visible region are much higher than that of the ruthenium complex N719 and I_3^- (25,000 $dm^3mol^{-1}cm^{-1}$, *ca.* 380 nm).[23,24] A higher molar

extinction coefficient means a higher light harvesting ability in the wavelength region of 300-450 nm compared with N719 and I_3^-. Hence, the photon lost due to the light absorption by I_3^- will be suppressed by employing the prepared compound as a co-sensitizer due to the competition between them and I_3^- to absorb light.

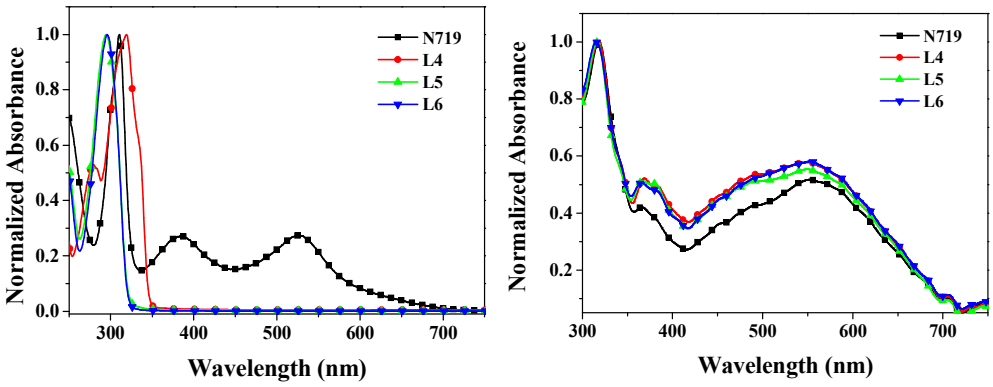

Fig. 1 UV-visible absorption spectra of prepared compounds and N719 (a) in ethanol, (b) on TiO_2 film.

Table 1 Experimental data for spectral and electrochemical properties of BPPI

Sensitizers	λ_{abs} (nm)[a]	ε ($dm^3mol^{-1}cm^{-1}$)[a]	E_{ox} (V vs SCE)[b]	$E_{0\text{-}0}$ (eV)[c]	E_{HOMO} (eV)[d]	E_{LUMO} (eV)[d]
L4	318	83760	0.65	2.90	-5.05	-2.15
L5	294	78962	0.70	2.91	-5.10	-2.19
L6	295	70125	0.71	2.91	-5.11	-2.19
N719	310, 385, 525	68254, 18560, 18710	1.05	1.60	-5.45	-3.85

[a] Absorption and emission spectra were recorded in ethanol solution (3×10^{-4} M) at room temperature.
[b] The first oxidation potentials of compounds were obtained by CV measurement.
[c] Optical band gap calculated from intersection between the absorption and emission spectra.
[d] The values of E_{HOMO} and E_{LUMO} were calculated with the following formula:
$E_{HOMO} = -(E^{ox}_{onset} + 4.4)(eV)$; $E_{LUMO} = E_{HOMO} + E_{0\text{-}0}$
where $E_{0\text{-}0}$ is the absorption edge of the dyes.

To further investigate whether the prepared compounds are suitable for use in DSSCs, the absorption spectra of L4/N719, L5/N719 and L6/N719 co-sensitized TiO_2 films are recorded and shown in Fig. 1b. As shown in Fig. 1b, the absorption of N719 on TiO_2 film in visible light region is remarkably broadened due to the electronic coupling of the dyes on the TiO_2 surface.[25] When N719 was combined with L4, L5 and L6, respectively, its absorption on TiO_2 film was enhanced in the region of 300-700 nm. This was partly because the adsorption of prepared compounds could compensate for that of N719, and on the other hand,

the emission spectra indicate that there is a synergy effect between N719 and prepared compounds. As shown in Fig. 2. All of them exhibit strong luminescence in the region of wavelength 300-500 nm, and it is worth to note that all of the emission spectra of L4, L5 and L6 overlap with the excitation spectra of N719 inordinately, which is a prerequisite for the effective electronic excitation energy transfer. This indicates that N719 could synchronously accept the energy from the incident light and the excited compounds, which will enhance the spectra response of N719 in the region of 300-700 nm.

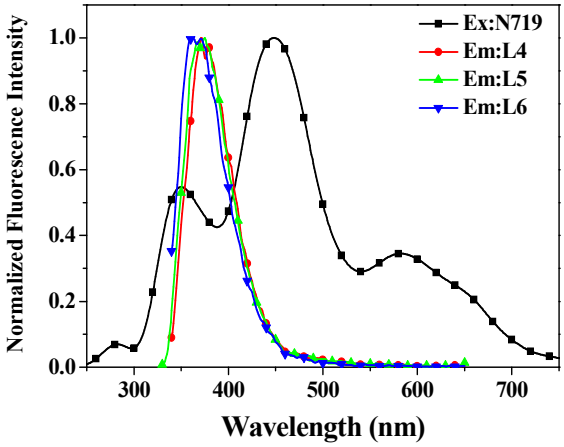

Fig. 2 The emission spectra of L1, L2 and L3 in ethanol solution.

From the adsorption spectra it could be predicted that employing L4, L5 or L6 into DSSCs as a co-sensitizer is a effectively way to enhance its performance by overcoming the deficiency of N719 absorption in the low wavelength region, offsetting competitive visible light absorption of I_3^- and enhancing the spectral responses of the co-sensitized TiO_2 film.

3.2 Electrochemical properties of L4, L5 and L6

Energy matching is crucial in selecting sensitizers for DSSCs. Therefore, in order to evaluate if there are favorable energy offsets of the prepared compounds with respect to the TiO_2 film and the electrolyte, the HOMO and LUMO energy levels of L4, L5 and L6 were investigated by cyclic voltammetry (CV) measurement in a three-electrode cell and an electrochemistry

workstation. The experimental data are summarized in Table 1. As estimated from the intersection of the absorption and emission spectra, the excitation transition energy ($E_{0\text{-}0}$) of L4, L5 and L6 are 2.90, 2.90 and 2.90 eV, respectively. Consequently, the HOMO values of L4, L5 and L6 are calculated based on their first redox potentials as -5.05, -5.10 and -5.11 eV, respectively, and the LUMO levels of L4, L5 and L6 calculated from $E_{HOMO} + E_{0\text{-}0}$, are -2.15, -2.19 and -2.18 eV, respectively.[26] The HOMO and LUMO energy levels of L4, L5 and L6 are shown in Scheme 3. It shows that the energy levels of the prepared compounds are appropriate for the DSSCs system containing TiO_2. The LUMO levels lied above the conduction band of the TiO_2 semiconductor (-4.40 eV vs vacuum), indicating efficient electron injection, and the HOMO energy levels lied below the I^-/I_3^- redox electrolyte (-4.60 eV vs vacuum) which is further improved negatively about 0.3 V by adding additives such as 4-tert-butyl pyridine (TBP) to the I^-/I_3^- redox electrolyte,[27] providing sufficient driving force for dye regeneration.[28]

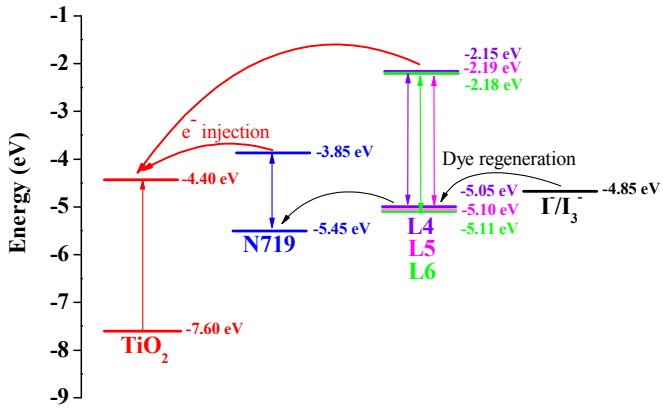

Scheme 3 Schematic energy diagram of HOMO and LUMO for compounds compared to the energy levels calculated for TiO_2.

3.3 Photovoltaic properties of DSSCs

The co-sensitized DSSCs are fabricated followed a stepwise co-sensitization procedure by sequentially immersing the TiO_2 electrode (with thickness of *ca.* 10 um) in separate solution of N719 and prepared compound. In one case, the TiO_2 electrode was firstly immersed into

the L4 solution and secondly in the N719 solution resulting in device L4/N719/TiO_2. The optimum soaking time for the TiO_2 photoanode film in L4 and N719 was found to be 2 h and 12 h, respectively. The devices of L5/N719/TiO_2 and L6/N719/TiO_2 are fabricated in the same way. For comparison purpose, devices sensitized by the individual dyes of N719 were also fabricated under the same experimental conditions.

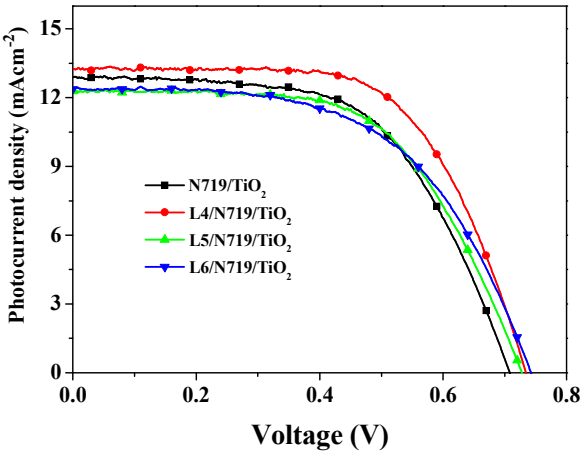

Fig. 3 *J-V* curves for DSSCs based on different photoelectrodes under irradiation.

Table 2 *J-V* performance of DSSCs based on different photoelectrodes

					Dye loading amout (10^{-7} mol cm^{-2})		
Photoelectrode	J_{sc} (mAcm^{-2})	V_{oc} (V)	*FF*	η (%)	N719	L (4, 5 or 6)	Total
N719/TiO_2	12.90	0.71	0.59	5.37	1.21	--	1.21
L4/N719/TiO_2	13.27	0.73	0.63	6.16	1.18	0.35	1.53
L5/N719/TiO_2	12.28	0.73	0.60	5.33	1.19	0.33	1.52
L6/N719/TiO_2	12.38	0.74	0.57	5.21	1.19	0.34	1.53

The current-voltage (*J-V*) characteristic of the DSSCs devices based on N719/TiO_2, L4/N719/TiO_2, L5/N719/TiO_2 and L6/N719/TiO_2 photoanodes under illumination (AM 1.5 G, 100 mWcm^{-2}) are shown in Fig. 3, and the corresponding cells performance are summarized in Table 2. The individually N719 sensitized device was found to exhibit η value of 5.37% (with J_{sc} = 12.90 mAcm^{-2}, V_{oc} = 0.71 V, and *FF* = 0.59), while the co-sensitized solar cell devices L4/N719/TiO_2, L5/N719/TiO_2 and L6/N719/TiO_2 showed η value of 6.16% (with J_{sc} = 13.27 mAcm^{-2}, V_{oc} = 0.73 V, and *FF* = 0.63), 5.33% (with J_{sc} = 12.28 mAcm^{-2}, V_{oc} = 0.73 V, and *FF* = 0.60), and 5.21% (with J_{sc} = 12.38 mAcm^{-2}, V_{oc} =

0.74 V, and FF = 0.57), respectively. The J_{sc} of L4/N719 co-sensitized solar cell is higher than that of cell individually sensitized by N719, while the J_{sc} of L5/N719 and L6/N719 co-sensitized solar cells are lower than that of cell individually sensitized by N719. However, the V_{oc} increased in all the co-sensitized solar cell devices. The η is in the order of L4/N719/TiO_2 > N719/TiO_2 > L5/N719/TiO_2 > L6/N719/TiO_2, which indicated that different donor group make the co-sensitized performance much different.

It is well-known that the amount of dye loading to the photoanode can strongly affect the J_{sc}. The amounts of absorbed dye were measured by desorbing the dye from the dye-sensitized films in a 0.1 M NaOH solution in water and ethanol (1:1, V/V), and the results are listed in Table 2. As shown in Table 2, the amount of dye loading for N719/TiO_2 photoanodes is 1.21×10^{-7} mol cm^{-2}. And for co-sensitized photoanodes, the loading amount of N719 decreased slightly. This can be attributed to that N719 adsorbed at the Brønsted acid sites of the TiO_2 surface (the sites of hydroxyl groups bound to Ti atoms) *via* dehydration reactions and the prepared pyridine-anchor co-sensitizer was confirmed to adsorb preferentially at the Lew acid sites of the TiO_2 surface (the sites of exposed Ti atoms). However, competitive adsorption still occurs between N719 and prepared co-sensitizers on the Brønsted acid sites of the TiO_2 surface. The total amounts of dye absorption increased after co-sensitization, and the improvement of J_{sc} in co-sensitized solar cells of L4/N719/TiO_2 is mainly attributed to the increase of total amount of dye adsorption. However, although the total amounts of dye absorption increased after co-sensitization with L5 and L6, the J_{sc} value of L5/N719 and L6/N719 co-sensitized solar cells are still lower than individual N719 sensitized solar cells. This means that the amount of dye loading is not the only factor to affect J_{sc}, and this further confirmed that different donor group in

co-sensitizer also make the co-sensitized performance much different.

3.4 IPCE spectra of DSSCs

The different η value of co-sensitized solar cell compared with the individually N719 sensitized devices, is attributed to the different photovoltaic parameters J_{sc} and V_{oc}. Particularly, the changed J_{sc} value is ascribed to the different IPCE response of the cells, since they are related by the equation:

$$J_{sc} = \int e\phi_{\text{ph.AM1.5G}}(\lambda)d\lambda$$

where e is the elementary charge and $\phi_{\text{ph.AM1.5G}}$ is the photon flux at AM 1.5.[29]

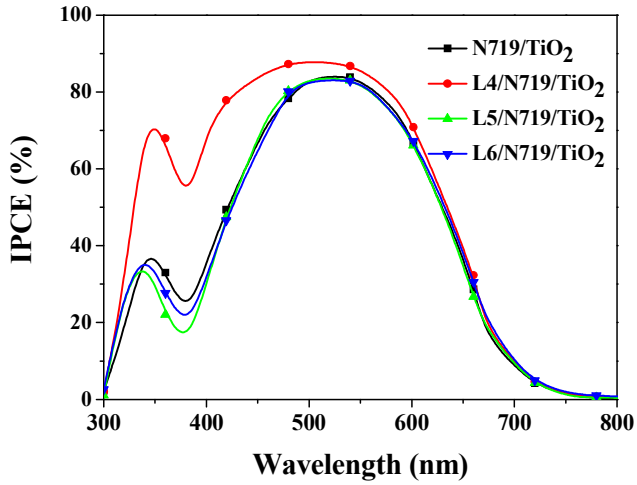

Fig. 4 IPCE spectra of DSSCs based on single N719 sensitized and co-sensitized photoelectrodes.

The IPCE spectra of different devices were collected in Fig. 4. The DSSCs containing only N719 dye has a broad IPCE spectrum from 300-750 nm but a decrease in the wavelength range of 340-450 nm, which is due to the competitive light absorption between I_3^- and N719. When L4 is used as co-sensitizer, not only this decrease is restored, but also the IPCE spectrum in the whole visible region is enhanced. This is attributed to the fact that L4 has attached to the TiO_2 surface effectively and contributed to the electron injection into the conduction band of the TiO_2. This means the co-sensitization of N719 and L4 has a

significant synergy and compensatory effect on light harvesting, electron injection and collection on TiO_2. However, when L5 and L6 are used as co-sensitizers, the IPCE spectrum in the whole visible region is not changed too much but a little decrease in the region of 300-450 nm. This make the J_{sc} value lower than N719 individually sensitized solar cells. The varied IPCE response of DSSCs may caused by the different donor group of L4, L5 and L6. When prepared with 1,2-diaminocyclohexane (L5) and 1,4-butanediamine (L6), the electron donor capability of donor groups are much weaker and the electron can not be injected effectively; While when prepared with 1,2-diaminobenzene (named L4), it is opposite.

3.5 Transient absorption spectroscopy (TAS) of DSSCs

In order to investigate the charge injection dynamics in different DSSCs and further understand the underlying causes which result in different short circuit current density (J_{sc}), Transient absorption spectroscopy (TAS) was employed to characterize co-sensitized and single N719 sensitized solar cells. Transient absorption spectroscopy is widely used to directly observe the electron injection process in dye-sensitized semiconductor films, and the reaction mechanism has been understood deeply as a function of the sensitizer dye, semiconductor, and environment. Also, co-sensitizers are known to affect the electron injection dynamics. The TA spectra of N719/TiO_2, L4/N719/TiO_2, L5/N719/TiO_2 and L6/N719/TiO_2 with the addition of an iodide-based electrolyte at 500 ps are shown in Fig. 5. The spectra show negative ground state bleaching (GSB) features, which result from a decrease in absorption in the excited dye, less than 620 nm (>2.0 eV). The spectra are dominated by a broad photo-induced absorption (PA) band, which results from increased absorption of the excited dye, greater than 620 nm (<2.0 eV). This broad PA band is the convolution of two PA spectral features. We attribute one PA feature to the absorption of the

excited-state dye (dye*) at approximately 650 nm, and the other to the absorption of the oxidized-dye (dye^+) at approximately 760 nm. The oxidized-dye is formed after charge injection occurs, and is therefore a probe of the ultrafast charge injection dynamics in DSSCs.[30,31] It is important to note in Fig. 5 that after co-sensitization with L4, L5 and L6, there is a increase in the PA signal at 650 nm (dye*), which indicates that more dye are excited after co-sensitization. This further confirms that there is a synergy effect between prepared co-sensitizer and N719, and the co-sensitizer could help to excite N719 by transferring its excited energy to N719 molecules. However, the situation of PA signal at 760 nm (dye^+) is quite different, which indicates that the charge injection was not the same after co-sensitization with different co-sensitizer and resulted in various J_{sc}. The PA signal at 760 nm (dye^+) increased after co-sensitized with L4, which indicates a better charge injection, and therefore it obtained a higher J_{sc} value. As for L5 and L6, the PA signal at 760 nm (dye^+) decreased after co-sensitization, which indicates a worse charge injection, and resulted in a lower J_{sc} value. The different charge injection is mainly caused by the molecular structure of L4, L5 and L6 with different donor groups.

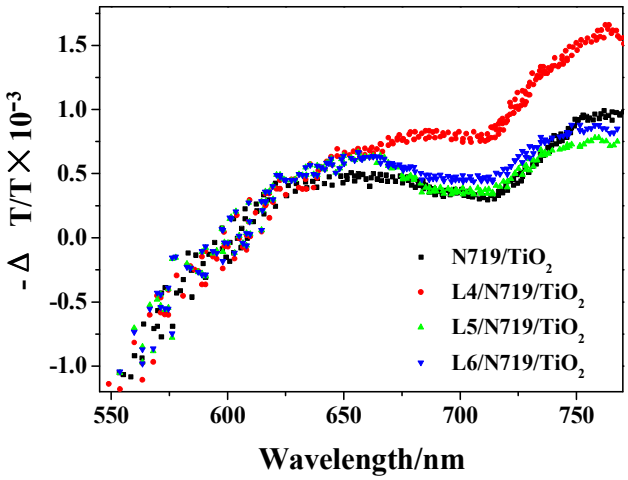

Fig. 5 Transient absorption spectra of co-sensitized and N719 sensitized solar cells.

3.6 Electrochemical impedance spectroscopy (EIS)

In an effort to understand the enhancement of the V_{oc} value in the co-sensitized solar cell and to investigate the kinetics of recombination processes, electrochemical impedance spectra (EIS) of devices based on different photoelectrodes were measured in dark by applying a forward bias of -0.75 V.[32,33] In the dark, the DSSCs behave as a leaking capacitor. Upon forward bias, the electrons are injected from the FTO substrate into the TiO_2 and the film is charged by electron propagation through the mesoscopic TiO_2 network. Meanwhile, a fraction of the injected conduction band electrons are lost by the reduction of I_3^- ions present in the electrolyte. Therefore, we could measure impedance spectra of DSSCs in the dark to study the electrons recombination from the conduction band of TiO_2 to I_3^- ions.

In dark conditions, as shown in Fig. 6a, the three semicircles located in high, middle and low frequency regions (left to right) of Nyquist plots are attributed to the redox reaction at the Pt counter electrode and the electron transfer at the TiO_2/dye/electrolyte interface and charge transfer in the electrolyte (Nernst diffusion).[34-36] Therefore the larger semicircle observed in middle frequency region represents the resistances of the charge transfer from the TiO_2 to the electrolyte (back recombination resistance R_{rec}). The radius of this semicircle increase after co-sensitized with prepared compounds, indicating an increase of R_{rec}. A large R_{rec} means the small charge recombination rate and vice versa. The radius of the semicircle observed in middle frequency range lies in the order of L6/N719/TiO_2 > L5/N719/TiO_2 > L4/N719/TiO_2 > N719/TiO_2, indicating sequence of R_{rec} at the TiO_2/dye/electrolyte interface. The increased value of R_{rec} for DSSCs implies the retardation of the charge recombination between injected electron and I^-_3 ions in the electrolyte, with a consequent increase of V_{oc}. This appears to be consistent with the larger V_{oc} values sequence.

The electron lifetime (τ_e) in different devices were calculated from the Bode phase plots of the EIS spectra of different solar cells (Fig. 6b), according to the relationship:

$$\tau_e = \frac{1}{2\pi f_{\max}}$$

where $f_{\max}$ is the frequency at the maximum of the curve in the intermediate frequency region in Bode phase plot. The electron lifetime (τ_e) for the devices co-sensitized with L4, L5 and L6 was found to be 11.0, 11.2, 12.6 ms, respectively, which are all longer than that of individually N719 sensitized device. This difference might be expected, since the adsorption of prepared compound may form a better dye coverage to help to passivate the TiO_2 surface or form an insulating molecular layer composed of prepared compound and N719 molecules and thus reduces the recombination due to electron back-transfer between TiO_2 and I_3^-.

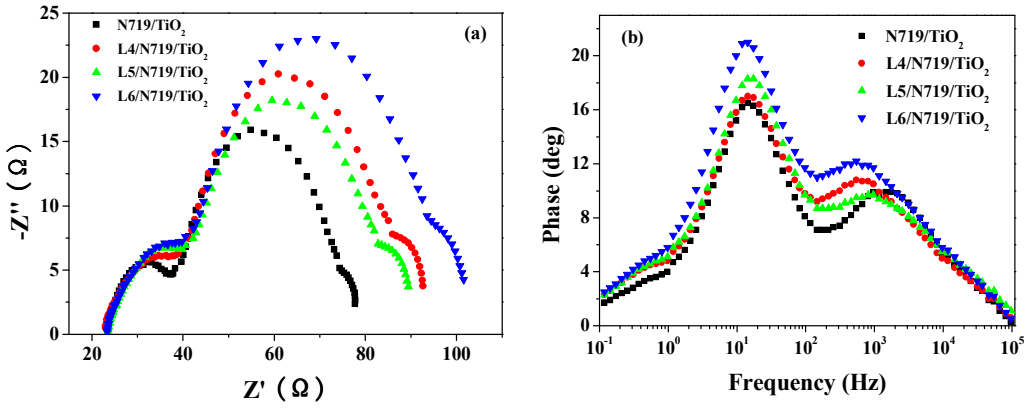

Fig. 6 (a) Nyquist plots (b) Bode plots of EIS for DSSCs based on different photoelectrodes measured in dark conditions.

Furthermore, to get the information about the electron transport mechanism in different devices, their electrochemical impedance spectra (EIS) were also measured under standard AM 1.5 G solar irradiation by applying a forward bias of -0.75V. Under light illumination, EIS was utilized to analyze the electron transport resistance at the TiO_2/dye/electrolyte interface for its significance on the efficiency of DSSCs.[37-39] As shown in Fig. 7a, the three

semicircles located in high, middle and low frequency regions (left to right) are attributed to the electrochemical reaction at the Pt/electrolyte interface, the electron transfer at the TiO_2/dye/electrolyte interface and charge transfer in the electrolyte (Nernst diffusion).[34-36] The radius of the large semicircle located in middle frequency regions in the Nyquist plots changed after co-sensitized with prepared compounds, and the values are in the order of L4/N719/TiO_2 < N719/TiO_2 < L6/N719/TiO_2 < L5/N719/TiO_2, which indicates a decrease of the electron transfer impedance (R_{ct}) and a increase of electron transfer rate at this interface after co-sensitization with L4; while after co-sensitized with L5 and L6, the electron transfer impedance (R_{ct}) increase and the electron transfer rate decrease at this interface. This is also the reason why the J_{sc} value for L4/N719 is higher and lower for L5/N719 and L6/N719.

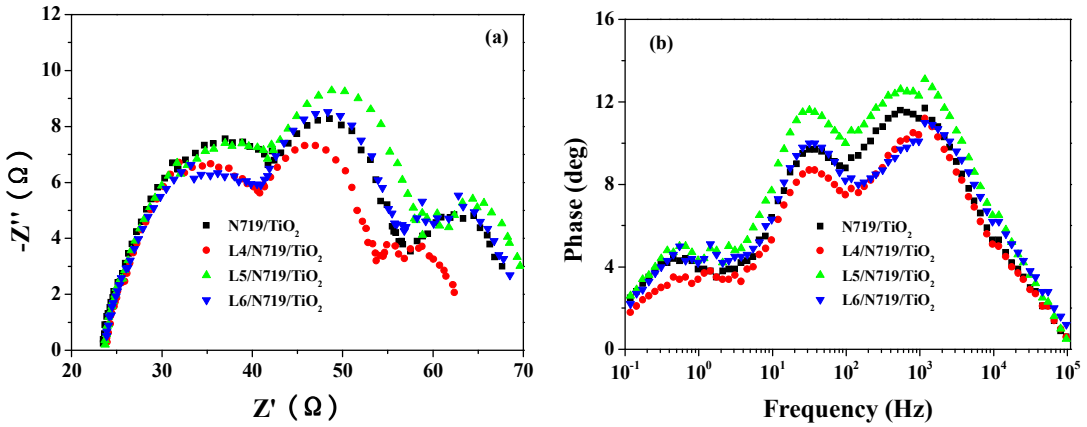

Fig. 7 (a)Nyquist plots (b) Bode plots of EIS for DSSCs based on different photoelectrodes measured under standard AM1.5 G solar irradiation.

The electron transport time (τ_d) is a measure of the average time taken by the injected electron to reach the collecting FTO electrode; a faster electron transport time is associated with a higher photocurrent.[40] It could also be calculated from the Bode phase plots of the EIS spectra of different solar cells (Fig. 7b), according to the relationship:

$$\tau_d = \frac{1}{2\pi f_{\max}}$$

where f_{max} is the frequency at the maximum of the curve in the intermediate frequency region in Bode phase plot. The calculated electron transport time (τ_d) for the devices co-sensitized with L4/N719, L5/N719 and L6/N719 are 4.39, 5.40 and 4.78 ms, respectively. Compared with the electron transport time of N719 (4.5 ms), it is shorter for L4/N719 co-sensitized device and longer for L5/N719 and L6/N719 co-sensitized solar cells. Longer electron transport time means slower electron transport rate and lower J_{sc} value and vice versa. Meanwhile, longer transport time also make it hard for electron to transport to FTO collector, this is afford to the unchanged IPCE response of L5 and L6. The shorter electron transport time for L4/N719 co-sensitized device is attributed to the better electron transport properties of L4, its better coverage on TiO_2 surface and better synergy effect with N719, which caused by its special donor group.

3.7 Dark current measurement

Dark current measurement of DSSCs is considered as a qualitative technique to describe the extent of the back electron transfer.[41,42] It could provide useful information regarding the back electron transfer process by making a comparison of dark current between the investigated cells. The dark current-voltage (*J-V*) measurements of different devices are presented in Fig. 8. It shows that the dark current is lower for the co-sensitized system compared with that of single N719 sensitized DSSC, which is in the order of L6/N719/TiO_2 < L4/N719/TiO_2 < L5/N719/TiO_2 < N719/TiO_2. The reduction of the dark current demonstrated that L4, L5 and L6 successfully suppress the electron back reaction with I_3^- in the electrolyte by forming a compact layer with N719, giving rise to V_{oc}, which is consistent with the results of EIS in dark condition.

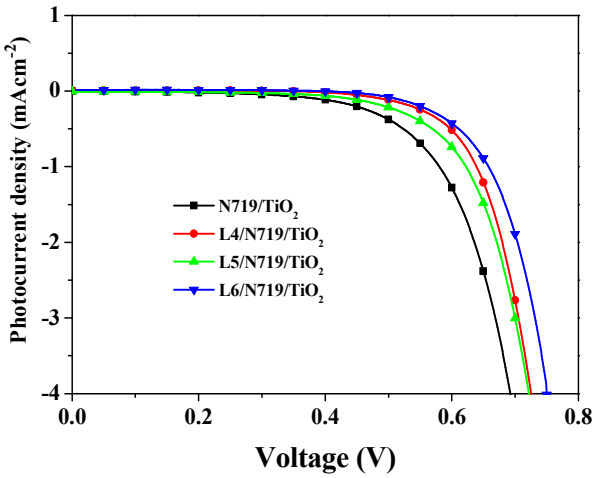

Fig. 8 *J-V* curves for DSSCs based on different photoelectrodes in dark.

3.8 Open-circuit voltage decay (OCVD)

The OCVD technique is a powerful tool to study interfacial recombination processes in the TiO_2 DSSCs between injected electrons and the electrolyte. It can provide some quantitative information on the electron recombination velocity in DSSCs.[43,44] The OCVD decay curves of the DSSCs based on different photoelectrode are shown in Fig. 9a. It was observed that the OCVD response of the DSSC with co-sensitized photoelectrode was much slower than that individually sensitized by N719, especially in the shorter time domain (within 30 s). Since the decay of the V_{oc} reflects the decrease in the electron concentration, which is mainly caused by the charge recombination,[45] the cell sensitized by the prepared compound has a lower electron recombination rate than that of the cell individually sensitized by N719.

Under the dark and open-circuit state conditions, electron lifetime (τ_e) was used to quantify the extent of electron recombination with the redox electrolyte. τ_e was calculated with the OCVD results in Fig. 9a according to the following equation:

$$\tau_e = -\frac{k_B T}{e}\left(\frac{dV_{oc}}{dt}\right)^{-1} \qquad (3)$$

where k_B is the Boltzmann constant, T is absolute temperature, e is the electronic charge, and

dV_{oc}/dt is the derivative of the transient open-circuit voltage.[46] Fig. 9b compares the results of the dependence of τ_e on the open-circuit voltage for co-sensitized and N719sensitized solar cells. It can be clearly seen that the electron lifetime of the co-sensitized cell was longer than that of the cell individually sensitized by N719 at any given V_{oc} value. The difference in OCVD was mainly due to the blocking effect of the compact layer made by prepared compound and N719. This suggests that the electrons injected from excited dye can survive longer and hence can facilitate electron transport without undergoing many losses at the bare FTO surface. Therefore, employing the prepared compound as a co-sensitizer is able to reduce the photoelectron recombination speed and prolong the lifetime of the photoelectrons.

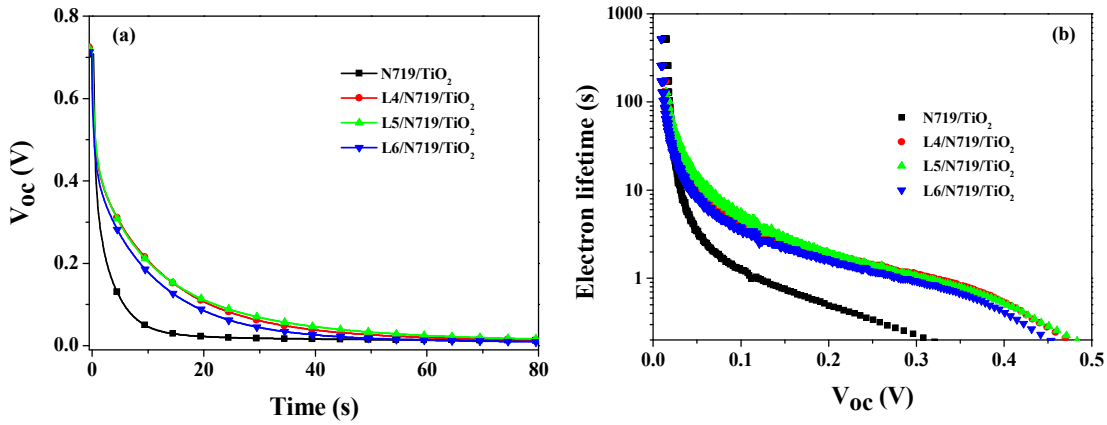

Fig. 9 (a) Open-circuit voltage decay curves of the DSSCs based on different photoelectrodes. (b) Comparison of electron lifetime as a function of open-circuit voltage of DSSCs based on different photoelectrodes.

3.9 Relationship between molecular structures and DSSC performance

Moreover, when the molecular structures of the prepared compounds are taken into account, it is found that introduction of different donor groups to bis(6-methoxylpyridin-2-yl) substituted co-sensitizer has important effect on the performance of DSSCs. The performance of co-sensitized DSSCs compared with that of single N719 sensitized DSSCs is

in the order of L4/N719/TiO_2 > N719/TiO_2 > L5/N719/TiO_2 > L6/N719/TiO_2. As show in Scheme 2, when 1,2-diaminobenzene, 1,2-diaminocyclohexane and 1,4-butanediamine is used to prepare co-sensitizer, respectively, three bis(6-methoxylpyridin-2-yl) substituted co-sensitizers of L4, L5 and L6 with different donor group are obtained. It is found that the rigidity and co-planarity of L4, L5 and L6 are in the order of L4 > L5 > L6. Better rigidity and co-planarity means easier electron transport and higher electrochemical properties. Herein, L4 shows better co-sensitization performance and the η value of L4/N719 co-sensitized solar cell is higher than that of N719 individually sensitized solar cell. However, the semi-rigid co-sensitizer L5 and flexible co-sensitizer L6 do not show better co-sensitization performance. Although these three co-sensitizers are all suitable to be used in N719 sensitized solar cells considered from optical property and energy levels, the rigidity also plays an important role in the co-sensitization process. A rigid molecule could ensure the regular and compact arrange during adsorption, which is benefit for electron transport; while the semi-rigid and flexible molecules could hardly to ensure this due to molecular rotation. On the other hand, the co-planarity of co-sensitizer molecule also affects the co-sensitization process. Better co-planarity usually companied with better conjugation, which better for electron transport. This is also the reason why L4 show better performance than L5 and L6. The difference of donor group in co-sensitizer molecule makes the molecular structure different, resulting in different rigidity, co-planarity and conjugation. All of these structure properties make the co-sensitization performance in the order of L4/N719/TiO_2 > N719/TiO_2 > L5/N719/TiO_2 > L6/N719/TiO_2. The molecular structure of co-sensitizer has important effect on the performance of co-sensitized solar cells. Therefore, it is critical to choose a suitable molecular structure in selection of co-sensitizers.

4. Conclusions

In conclusion, the synthesized bis(6-methoxylpyridin-2-yl) substituted pyridine-anchor co-sensitizers are suitable to be employed in N719 sensitized solar cells as co-sensitizer. However, as the donor group is different, the rigidity, co-planarity and conjugation are changed, which are in the order of L4 > L5 > L6. Better rigidity and co-planarity means easier electron transport and higher electrochemical properties. Herein, L4 shows better co-sensitization performance and the η value of L4/N719 co-sensitized solar cell is higher than that of N719 individually sensitized solar cell. However, the semi-rigid co-sensitizer L5 and flexible co-sensitizer L6 do not show better co-sensitization performance. The co-sensitization performance is in the order of L4/N719/TiO_2 > N719/TiO_2 > L5/N719/TiO_2 > L6/N719/TiO_2. A short circuit current density of 13.27 mA cm^{-2}, an open circuit voltage of 0.73 V and a fill factor of 0.63 corresponding to an overall conversion efficiency of 6.16% under AM 1.5G solar irradiation were achieved when rigid L4 was used as co-sensitizer, which is 30% higher than that for DSSCs only sensitized by N719 (5.37%) under the same condition. The molecular structure of co-sensitizer has important effect on the performance of co-sensitized solar cells and it is critical to choose a suitable molecular structure in selection of co-sensitizers.

Acknowledgements

This work was supported by National Natural Science Foundation of China (Grant 21171044, 21371040 and 21571042), the National key Basic Research Program of China (973 Program, No. 2013CB632900), the Fundamental Research Funds for the Central Universities (Grant No. HIT. IBRSEM. A. 201409), and Program for Innovation Research of Science in Harbin Institute of Technology (PIRS of HIT No. A201418, A201416 and B201414).

References

1 A. Hagfeldt, G. Boschloo, L. Sun, L. Kloo and H. Pettersson, Chem. Rev., 2010, **110**, 6595–6663.

2 B. O'Regan and M. Grätzel, Nature, 1991, **353**, 737–740.

3 U. Mehmood, I. A. Hussein, K. Harrabi, M. B. Mekki, S. Ahmed and N. Tabet, Solar Energy Materials and Solar Cells, 2015, **140**, 174–179.

4 A. Yella, H. W. Lee, H. N. Tsao, C. Y. Yi, A. K. Chandiran, M. K. Nazeeruddin, E. W. G. Diau, C. Y. Yeh, S. M. Zakeeruddin and M. Gratzel, Science, 2011, **334**, 629-634.

5 G. D. Sharma, P. A. Angaridis, S. Pipou, G. E. Zervaki, V. Nikolaou and R. Misra, Organic Electronics, 2015, **25**, 295–307.

6 G. D. Sharma, M. S. Roy and S. P. Singh, J. Mater. Chem., 2012, **22**, 18788–18792.

7 L. Y. Han, A. Islam, H. Chen, C. Malapaka, B. Chiranjeevi, S. F. Zhang, X. D. Yang and M. Yanagida, Energy Environ. Sci., 2012, **5**, 6057-6060.

8 H. Ozawa, R. Shimizu and H. Arakawa, RSC Adv., 2012, **2**, 3198–3200.

9 M. Mojiri-Foroushani, H. Dehghani and N. Salehi-Vanani, Electrochim. Acta, 2013, 92, 315–322.

10 P. J. Holliman, M. Mohsen, A. Connell, M. L. Davies, K. Al-Salihi, M. B. Pitak, G. J. Tizzard, S. J. Coles, R. W. Harrington, W. Clegg, C. Serpa, O. H. Fontes, C. Charbonneau and M. J. Carnie, J. Mater. Chem., 2012, **22**, 13318-13327.

11 K. M. Lee, Y. C. Hsu, M. Ikegami, T. Miyasaka, K. R. J. Thomas, J. T. Lin and K. C. Ho, J. Power Sources, 2011, **196,** 2416-2421.

12 S. Q. Fan, C. Kim, B. Fang, K. X. Liao, G. J. Yang, C. J. Li, J. J. Kim and J. Ko, J. Phys. Chem. C, 2011, **115**, 7747-7754.

13 G. D. Sharma, D. Daphnomili, K. S. V. Gupta, T. Gayathri, S. P. Singh, P. A. Angaridis, T. N. Kitsopoulos, D. Tasis and A. G. Coutsolelos, RSC Adv., 2013, **3**, 22412-22420.

14 Z. Wu, Y. Wei, Z. An, X. Chen and P. Chen, *Bull. Korean Chem. Soc.*, 2014, **35**, 1449-1452.

15 S. Chang, H. Wang, L. T. L. Lee, S. Zheng, Q. Li, K. Y. Wong, W. K. Wong, X. Zhu, W. Y. Wong, X. Xiao and T. Chen, J. Mater. Chem. C, 2014, **2**, 3521-3526.

16 Y. Harima, T. Fujita, Y. Kano, I. Imae, K. Komaguchi, Y. Ooyama and J. Ohshita, J. Phys. Chem. C, 2013, **117**, 16364–16370.

17 Y. Ooyama, S. Inoue, T. Nagano, K. Kushimoto, J. Ohshita, I. Imae, K. Komaguchi and Y. Harima, Angew. Chem. Int. Ed., 2011, **50**, 7429–7433.

18 Y. Ooyama, N. Yamaguchi, I. Imae, K. Komaguchi, J. Ohshita and Y. Harima, Chem. Commun., 2013, **49**, 2548–2550.

19 D. Daphnomili, G. Landrou, S. P. Singh, A. Thomas, K. Yesudas, K. Bhanuprakash, G. D. Sharma and A. G. Coutsolelos, RSC Advances, 2011, **2**, 12899–12908.

20 L. G. Wei, Y. L. Yang, R. Q. Fan, Y. Na, P. Wang, Y. W. Dong, B. Yang and W. W. Cao, Dalton Transactions, 2014, **43**, 11361-11370.

21 L. G. Wei, Y. L. Yang, R. Q. Fan, Y. Na, P. Wang, Y. W. Dong and W. Zhou, Journal of Power Sources, 2015, **293**, 203-212.

22 P. Y. Reddy, L. Giribabu, C. Lyness, H. J. Snaith, C. Vijaykumar, M. Chandrasekharam, M. Lakshmikantam, J. H. Yum, K. Kalyanasundaram, M. Grätzel and M. K. Nazeeruddin, Angew. Chem. Int. Ed., 2007, **46**, 373–376.

23 D. B. Kunag, S. Ito, B. Wenger, C. Klein, J. E. Moser, R. Humphry-Baker, S. M. Zakeeruddin and M. Grätzel, J. Am. Chem. Soc., 2006, **128**, 4146–4154.

24 G. D. Sharma, S. P. Singh, R. Kurchania and R. J. Ball, RSC Adv., 2013, **3**, 6036–6043.

25 C. Y. Lin, C. F. Lo, L. Luo, H. P. Lu, C. S. Hung, E. W. G. Diau, J. Phys. Chem. C, 2009, **113**, 755–764.

26 C. M. Cardona, W. Li, A. E. Kaifer, D. Stockdale and G. C. Bazan, Adv. Mater., 2011, **23**, 2367–2371.

27 G. Boschloo, L. Halggman and A. Hagfeldt, J. Phys. Chem. B, 2006, **110**, 13144–13150.

28 K. R. Justin Thomas, Y. C. Hsu, J. T. Lin, K. M. Lee, K. C. Ho, C. H. Lai, Y. M. Cheng and P. T. Chou, Chem. Mater., 2008, **20**, 1830–1840.

29 A. Hagfeldt, G. Boschloo, L. Sun, L. Kloo and H. Pettersson, Chem. Rev., 2010, **110** , 6595–6663.

30 S. A. Haque, E. Palomares, B. M. Cho, A. N. M. Green, N. Hirata, D. R. Klug and J. R. Durrant, J. Am. Chem. Soc., 2005, **127**, 3456–3462.

31 S. E. Koops, B. C. O'Regan, P. R. F. Barnes and J. R. Durrant, J. Am. Chem. Soc., 2009, **131**, 4808–4818.

32 J. Bisquert, J. Phys. Chem. B, 2002, 106, 325–333.

33 J. Bisquert, A. Zaban, M. Greenshtein and I. Mora-Sero, J. Am. Chem. Soc., 2004, **126**, 13550–13559.

34 J. Bisquert, Phys. Chem. Chem. Phys., 2003, **5**, 5360–5364.

35 D. Kuang, S. Uchida, R. Humphry-Baker, S. M. Zakeeruddin and M. Grätzel, Angew. Chem. Int. Ed., 2008, **47**, 1923–1926.

36 N. Koide, A. Islam, Y. Chiba and L. Y. Han, J. Photochem. Photobiol. A Chem., 2006, **182**, 296–303.

37 C. P. Hsu, K. M. Lee, J. T. W. Huang, C. Y. Lin, C. H. Lee, L. P. Wang, S. Y. Tsai and K. C. Ho, Electrochimica Acta, 2008, **53**, 7514–7522.

38 K. E. Lee, M. A. Gomez, C. Charbonneau and G. P. Demopoulos, Electrochimica Acta, 2012, **67**, 208–215.

39 C. Y. Hsu, W. T. Chen, Y. C. Chen, H. Y. Wei, Y. S. Yen, K. C. Huang, K. C. Ho, C. W. Chu and J. T. Lin, Electrochimica Acta, 2012, **66**, 210–215.

40 M. Adachi, M. Sakamoto, J. T. Jiu, Y.Ogata and S. Isoda, J. Phys. Chem. B, 2006, **110**, 13872–13880.

41 A. Zaban, A. Meier and B. A. Gregg, J. Phys. Chem. B, 1997, **101**, 7985–7990.

42 S. Ito, P. Liska, P. Comte, R. Charvet, P. Pechy, U. Bach, L. Schmidt-Mende, S. M. Zakeeruddin, A. Kay, M. K. Nazeeruddin and M. Graetzel, Chem. Commun., 2005, **25**, 4351-4353.

43 J. Bisquert, A. Zaban, M. Greenshtein and I. Mora-Sero, J. Am. Chem. Soc., 2004, **126**, 13550-13559.

44 K. Fan, W. Zhang, T. Peng, J. Chen and F. Yang, J. Phys. Chem. C, 2011, **115**, 17213–17219.

45 H. Yu, S. Q. Zhang, H. J. Zhao, G. Will and P. R. Liu, Electrochim. Acta, 2009, **54**, 1319–1324.

46 A. Zaban, M. Greenshtein and J. Bisquert, ChemPhysChem, 2003, **4**, 859-864.

Effect of different donor group in bis(6-methoxylpyridin-2-yl) substituted co-sensitizer on the performance of N719 sensitized solar cells

Liguo Wei,[ab] Yulin Yang,*[a] Zhaoyang Zhu,[ac] Ruiqing Fan,*[a] Ping Wang,[a] Yuwei Dong[a] and Shuo Chen[a]

[a] *Department of Chemistry, Harbin Institute of Technology, Harbin 150001, P.R. China.*

[b] *College of Environmental and Chemical Engineering, Heilongjiang University of Science and Technology, Harbin 150022, P.R. China.*

[c] *Hubei Institute of Aerospace Chemotechnology, Xiangyang 441003, P.R. China.*

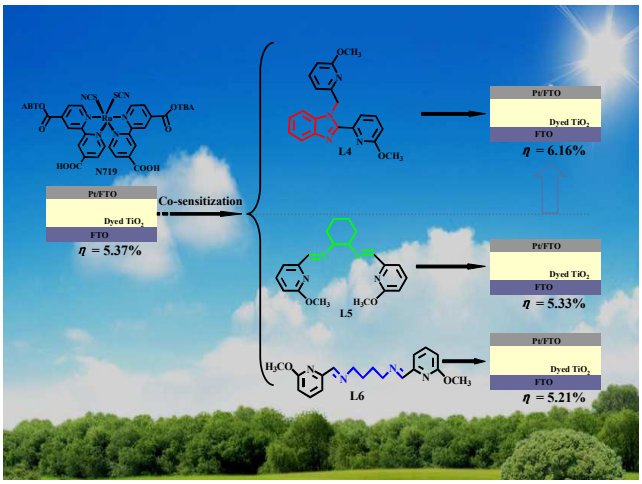

The donor group of co-sensitizer has important effect on the performance of co-sensitized solar cells.

To whom the correspondence should be addressed.

Prof. Yulin Yang and Ruiqing Fan

Department of Chemistry, Harbin Institute of Technology, Harbin 150001, P. R. China

Fax: +86-451-86418270

E-mail: ylyang@hit.edu.cn and fanruiqing@hit.edu.cn